Thermal cracking prediction for a squeeze casting process with an approach of multi-scale and multi-model coupling

zhan Zhao (1043575198@qq.com)
Taiyuan University of Technology
Yan LIU
Xiaofeng Niu
Tao-tao GE
Ming-yu ZHANG
Wei ZHOU
Pei-lin LUO

Research Article

Keywords: multi-model coupling, multi-scale calculation, squeeze casting, thermal crack prediction

Posted Date: March 15th, 2022

DOI: https://doi.org/10.21203/rs.3.rs-1436776/v1

Thermal cracking prediction for a squeeze casting process with an approach of multi-scale and multi-model coupling

Zhan ZHAO, Yan LIU, Xiao-feng NIU*, Tao-tao GE, Ming-yu ZHANG, Wei Zhou，Pei-lin LUO

School of Materials Science and Engineering, Taiyuan University of Technology, Taiyuan 030024,China

corresponding author e-mail :niuxiaofeng@tyut.edu.cn

Abstract

The smooth particle hydrodynamics (SPH) method is advantageous in tracking a free surface and a moving interface. This paper uses the SPH method to simulate the filling process of squeeze casting. The simulated temperature field at the end of filling was input into a finite element model (FEM) program to simulate the solidification process after squeeze casting. Due to the existence of a liquid phase, a solid phase, and a two-phase mushy zone in the solidification process after squeeze casting, the deformation behavior in the solidification process was modeled with a thermoelasto–viscoplastic constitutive model representing these different phases. In the RDG thermal cracking criterion based on the principle of dendrite gap complement, there are a strain rate term, a secondary dendritic spacing term, and a pressure term. These terms accurately describe the squeeze casting process. Therefore, the RDG criterion was used to predict thermal cracking. The strain rate term in the RDG criterion was calculated by the FEM. For the calculation of the secondary dendritic spacing, the temperature field during the solidification process is locally refined by the FDM method to complete the transition from the macroscale to the mesoscale; then the refinement results are imported into the phase field method for dendritic growth simulation. The results show that the method based on multi-model coupling has satisfactory prediction accuracy for the thermal cracking in the squeeze casting process. The combination of the phase field method and the RDG criterion provides a new approach to the simulation of thermal cracking defects. The prediction results show that the thermal cracking tendency increases with an increase in strain rate. However, the local position C of the bracket sample had a higher strain rate of 7.15/s, and a lower cooling rate of 2.96 K/s offset the effect of the high strain rate. As a result, a low thermal cracking tendency level of 1.13729 was obtained.

Keywords: multi-model coupling; multi-scale calculation; squeeze casting; thermal crack prediction

1. Introduction

Squeeze casting is a process combining the characteristics of pressurized casting and die forging. The metal liquid is put into an external die bore first, and then pushed into a mold cavity by a punch. After filling is finished, the punch continues to move to pressurize the metal liquid until the metal is completely solidified. The squeeze casting technology has been developed rapidly in the military industry since recent years. It solves the problem of direct shape forming without too much processing, and also offers good mechanical properties. This technology has been gradually applied in mass production to manufacture wheel hubs and brackets for military equipment. To pursue a more efficient process and a shorter production cycle, it is necessary to simulate the squeeze casting process.

The SPH method is called smooth particle hydrodynamics method. This method transforms a continuous medium into particles with virtual volumes and integrates physical properties on each particle. It utilizes interactions between particles to reflect the changing behavior of mass, energy, and momentum. The particles can move freely with the physical properties. In contrast, a meshed grid cannot move freely. Due to the advantages of the mathematical model, the SPH method can simulate large deformations and hence is suitable for simulating the casting filling process. Cleary[1] used the SPH method to simulate a three-dimensional filling process of high-pressure casting. He compared the SPH simulation result of filling with the result obtained by Magma and found that the SPH method can better capture key details of fluid motions and spillage compared to the FDM method, especially the relative velocity in narrow cross sections. Subsequently, Cleary[2] app lied the SPH method to die casting simulation of complex thin-wall parts and confirmed satisfactory accuracy of the SPH method in capturing details of high-throughput filling processes. The SPH method was used in this study to simulate the filling process of squeeze casting.

In the FEM, the computational domain is divided into a finite number of non-overlapping interconnected elements and nodes. The calculation accuracy of the FEM mainly depends on the user's meshing capability. Better meshing can provide more accurate simulation results. Chang[3] used the software Procast based on the FEM to evaluate the effects of squeeze casting parameters on casting quality. The parameters included gate speed, casting system design, and squeeze pressure. Li[4] used Procast to simulate the squeeze casting process of a gear box and predict shrinkage cavity and porosity defects, and determined technical parameters for the lowest shrinkage cavity ratio. The FEM has great advantages in stress and strain calculations, therefor, the FEM was used in this study to simulate the solidification process of squeeze casting. Because the deformation behavior in the squeeze casting process is very complex, including the elastic and plastic deformations of the solid phase and the elastic deformation and shear of the liquid phase, it is very important to choose a constitutive model. This paper analyzes an ADC12 aluminum alloy squeeze casting bracket. In the thermal deformation study of the aluminum alloy, most previous researchers used a hyperbolic sinusoidal rheological constitutive model proposed by Jonas[5], which contains a strain activation energy and a deformation temperature. This model can fit the temperature and the deformation rate accurately. Santhanam[6] added a strain term in the constitutive model to construct a thermoelasto–viscoplastic model

suitable for the thermal deformation of the aluminum alloy. However, his model does not consider the solid–liquid phase transition. Zhu and Han[7] proposed a constitutive model for squeeze casting, which includes the solid–liquid zone transition and the mechanical behavior of the metal shell during solidification. Their model was adopted in this study to simulate the interaction between deformation and solidification of the metal liquid.

Many scholars proposed different criteria based on various theories for the thermal cracking defect in the squeeze casting process. Hatami[8] and Clyne[9] proposed a thermal cracking criterion based on thermodynamics with two different stages: (1) solidification with feeding, and (2) solidification without feeding. The two stages are classified by solid phase volume fraction. The thermal cracking tendency is reflected by the ratio of the temperature interval of the stage and The time interval at which the alloy is in this stage. This criterion is not accurate and does not contain the micro mechanism of thermal cracking. Kou[10] proposed a thermal cracking criterion based on the solidification contraction angle. Thermal cracking occurs when the bulk increase in the liquid metal area caused by the strain cannot be balanced by flow feeding. This criterion only considers the mass balance without considering the effect of the microstructure on thermal cracking. Pappaz[11] proposed a RDG criterion based on solid mechanics and fluid mechanics. This criterion considers the pressure drop at the tip and the bottom of the dendrite. If the pressure drop is greater than a critical threshold value, the gap generated between dendrites cannot be compensated and hence cores of thermal cracking are formed. The RDG criterion considers the impacts of pressure, strain rate, and the microstructure. Therefore, it fits well the pressurized solidification process of squeeze casting.

The microstructure term, which is the secondary dendrite spacing, in the RDG criterion can be obtained by dendrite growth simulation. The phase field (PF) method can simulate the microstructure with differential equations by combining the solute diffusion, the order potential, and the thermodynamic driving forces. Kobayashi[12] proposed a PF model for the dendrite growth of pure materials. Almost all subsequent models using pure materials are based on Kobayashi's method. Warren[13] developed a comprehensive model to solve the heat dissipation equation and the solute diffusion equation during the solidification process. He introduced an order parameter (a phase field) to describe the interface region between the solid phase and the liquid phase, and obtained accurate simulation results of realistic secondary dendrite growth. Bailey[14] established a three-dimensional phase field model for a laser welding process, and compared it with a two-dimensional model. His model can predict the microstructure at any position in the laser welding process. In this paper, the equiaaxial dendrite growth model based on the phase field method proposed by Zaeem[15] is used to predict the secondary dendrite spacing in the RDG criterion.

In this paper, the approach of multi-model coupling is used to simulate the squeeze casting process by fully utilizing the advantages of multiple methods involved to accurately predict the thermal cracking tendency in the squeeze casting process. Meanwhile, the mesoscopic scale parameter of the secondary dendrite spacing was obtained by a multi-scale simulation using the phase field method. The combination of the phase field method and the RDG criterion provides a new approach to predict thermal cracking defects.

2. Numerical modeling

The SPH method was first used to simulate the filling process. Then, the result of filling at the moment of filling completion was input into the FEM program to continue the simulation of the solidification process. The phase field method was used to conduct the mesoscale simulation to obtain the secondary dendrite spacing term. The strain rate term was obtained by the FEM. These two terms were then input into the RDG criterion to predict thermal cracking.

2.1 Simulation model of the filling process

Because the SPH method has great advantages in tracking the free surface and the moving interface, this paper uses the SPH method to simulate the filling process of squeeze casting[16,17]. Then, the temperature field at the end of filling was input into the FEM to simulate the solidification process.

The approximate equation of the particles' function and its derivative are given by

$$\left\langle f(x_i)\right\rangle = \sum_{j=1}^{N} \frac{m_j}{\rho_j} f(x_j) W_{ij} \tag{1}$$

$$\left\langle \nabla \cdot f(x_i)\right\rangle = \sum_{j=1}^{N} \frac{m_j}{\rho_j} f(x_j) \cdot \nabla_i W_{ij} \tag{2}$$

Where i is the central particle, j is the particle in the supporting domain, and $\left\langle f(x)\right\rangle$ is a kernel approximation operator. N is the total number of the particles in the supporting domain of particle j, and W_{ij} is a smooth function reflecting the impact of particle j on particle i. ∇ is a gradient operator. The kernel function was selected as a cubic spline function. The three Navier–Stokes governing equations can be approximately transformed into the following forms via the SPH particles:

$$\frac{d\rho_i}{dt} = \sum_{j=1}^{N} m_j v_{ij}^{\beta} \cdot \frac{\partial W_{ij}}{\partial x_i^{\beta}} \tag{3}$$

$$\frac{dv_i^{\alpha}}{dt} = \sum_{j=1}^{N} m_j \left(\frac{p_i}{\rho_i^2} + \frac{p_j}{\rho_j^2}\right) \frac{\partial W_{ij}}{\partial x_i^{\alpha}} \tag{4}$$

$$\frac{de_i}{dt} = \frac{1}{2} \sum_{j=1}^{N} m_j \frac{p_i + p_j}{\rho_i \rho_j} \cdot \frac{\partial W_{ij}}{\partial x_i^{\beta}} \tag{5}$$

Eqs. (3) to (5) are the SPH expressions of the density equation, the momentum equation, and the energy equation, respectively, where ρ is density, v velocity, e internal energy of fluid microcluster, p pressure, α and β coordinate directions. The temperature field at the end of filling was input into the FEM as the initial condition at the start (t=0) of the solidification process.

In order to cope with the fluid dynamics environment of the filling process, an artificial viscosity term, as shown in Lattanzio[18], was introduced to convert the kinetic energy to the internal energy and prevent non-physical penetration caused by excessively small particle spacing. To further eliminate the phenomenon of tensile instability,

the artificial stress term proposed by Monaghan[19] was introduced to apply a repulsive force between particles that are excessively small to avoid excessive aggregation of particles. In this paper, the boundary force model adopts the virtual particle boundary force method proposed by Qiang[20], which uses multiple layers of virtual particles to implicitly represent the solid wall boundary. The virtual particles and the fluid particles interact directly through fluid mechanics control equations.

2.2 Simulation model of the solidification process

The results of the end of filling calculated by the SPH method were imported into the FEM program for solidification simulation. Since the SPH method integrates all information on the particles, while the FEM integrates part of information on nodes, if different partition scales are adopted, the errors in information transmission will be enlarged. Therefore, the developed approach in this paper uses a regional search method to seek the spherical space with the radius of the unit grid length with the FEM node as the center and also search the SPH particles within the range. The initial information of the FEM nodes was obtained by taking a weighted average on the coefficients that are equal to the distances between the SPH particles and the FEM nodes.

The motion equations of the FEM dynamic problem are given as follows[21]:

$$\mathbf{M}\ddot{a}(t) + \mathbf{C}\dot{a}(t) + \mathbf{K}a(t) = \mathbf{Q}(t) \tag{6}$$

$$\mathbf{M} = \sum_e \mathbf{M}^e \qquad \mathbf{M}^e = \int_{V_e} \rho \mathbf{N}^T \mathbf{N} dV \tag{7}$$

$$\mathbf{C} = \sum_e \mathbf{C}^e \qquad \mathbf{C}^e = \int_{V_e} \mu \mathbf{N}^T \mathbf{N} dV \tag{8}$$

$$\mathbf{K} = \sum_e \mathbf{K}^e \qquad \mathbf{K}^e = \int_{v_e} \mathbf{B}^T \mathbf{D} \mathbf{B} dV \tag{9}$$

$$\mathbf{Q} = \sum_e \mathbf{Q}^e \qquad \mathbf{Q}^e = \int_{V_e} \mathbf{N}^T \mathbf{f} dV + \int_{\Gamma_t^e} \mathbf{N}^T \mathbf{T} ds \tag{10}$$

Where $a(t)$ is node displacement, $\dot{a}(t)$ node velocity, and $\ddot{a}(t)$ node acceleration. $\mathbf{M}^e$, $\mathbf{C}^e$, $\mathbf{K}^e$, and $\mathbf{Q}^e$ are matrix vectors of element mass, damping, stiffness, and load, respectively. Because the displacement interpolation function used in Eq. (7) is the same as the function used in deriving the stiffness matrix, the element mass matrix in Eq. (7) is a uniform mass matrix. In order to facilitate the coupled simulation between the SPH particles and the finite elements, the FEM program uses the method of the concentrated mass matrix to lump the element mass on the node, as shown in Eq. (11) below:

$$(\mathbf{M}_l^e)_{ij} = \begin{cases} \sum_{k=1}^{n_e} (\mathbf{M}^e)_{ik} = \sum_{k=1}^{n_e} \int_{V_e} \rho \mathbf{N}^T \mathbf{N} dV & (j = i) \\ 0 & (j \neq i) \end{cases} \tag{11}$$

Where n_e is the number of element nodes. The lumped mass matrix $\mathbf{M}_l^e$ is a diagonal matrix, where the principal elements of each row are the sum of the principal elements of the uniform mass matrix.

The finite element form of the temperature field is given by

$$[C]\{\dot{\theta}\}+[K_T]\{\theta\}=\{F_T\} \tag{12}$$

Where $[C]$ is the total heat capacity matrix, $[K_T]$ the total heat conduction matrix, and $\{F_T\}$ the boundary temperature load vector. The parameters of $\{\theta\}$ and $\{\dot{\theta}\}$ are the temperature vector and its differential term, respectively.

The liquid metal solidifies under the pressure exerted by the punch. There is a solid metal shell near the mold wall of the cavity. The liquid metal is in the center of the cavity. There is also a mushy zone at the junction between the two phases in the cavity. Therefore, the mechanical behavior of the solidification process of squeeze casting is very complicated. Since metal deformation is affected by strain rate and temperature, the selection of the constitutive model is particularly important. The constitutive model described by Zhu and Han[7] is used in this paper to calculate the stress and strain in the FEM.

The strain increment within one time step is divided into three parts as follows:

$$\{\Delta\varepsilon\}=\{\Delta\varepsilon_{\mathrm{el}}\}+\{\Delta\varepsilon_{\mathrm{th}}\}+\{\Delta\varepsilon_{\mathrm{in}}\} \tag{13}$$

Where $\{\Delta\varepsilon_{el}\}$ is elastic strain increment, $\{\Delta\varepsilon_{th}\}$ thermal strain increment, and $\{\Delta\varepsilon_{in}\}$ inelastic strain increment.

The elastic strain increment is given by

$$\{\Delta\sigma\}=\Delta\left([D]\{\varepsilon_{\mathrm{el}}\}\right)=[D]\{\Delta\varepsilon_{\mathrm{el}}\}+[\Delta D]\{\varepsilon_{\mathrm{el}}\} \tag{14}$$

$$[D]=\frac{E(\theta)}{(1+\nu)(1-2\nu)}\begin{bmatrix} 1-\nu & \nu & \nu & 0 & 0 & 0 \\ & 1-\nu & \nu & 0 & 0 & 0 \\ & & 1-\nu & 0 & 0 & 0 \\ & Symmetry & & 1-2\nu/2 & 0 & 0 \\ & & & & 1-2\nu/2 & 0 \\ & & & & & 1-2\nu/2 \end{bmatrix} \tag{15}$$

The thermal strain increment is given by:

$$\{\Delta\varepsilon_{\mathrm{th}}^{t+\Delta t}\}=\left(\alpha_1\left(\theta^{t+\Delta t}\right)-\alpha_1\left(\theta^{t}\right)\right)\{1\quad 1\quad 0\}^{\mathrm{T}} \tag{16}$$

$$\alpha_1(\theta)=\sqrt[3]{\rho(\theta_0)/\rho(\theta)}-1 \tag{17}$$

Where $\rho(\theta_0)$ is the density at a reference temperature θ_0, and $\rho(\theta)$ is the density at that moment.

The inelastic strain increment is calculated in different sections. When the element is in a solid phase, it is believed that the yield stress is related to strain rate and temperature and obeys the thermoelasto–viscoplastic constitutive model as follows

$$\{\dot{\varepsilon}_{in}\} = \frac{3}{2}\dot{\bar{\varepsilon}}_{in}\frac{\{\sigma'\}}{\bar{\sigma}} \tag{18}$$

Where $\{\dot{\varepsilon}_{in}\}$ is the inelastic strain rate vector, and $\dot{\bar{\varepsilon}}_{in}$ is the equivalent inelastic strain rate. The measured temperature θ and the equivalent stress function $\bar{\sigma}$ are related to $\dot{\bar{\varepsilon}}_{in}$ as follows:

$$\dot{\bar{\varepsilon}}_{in} = f\left(\theta, \bar{\sigma}\right) \tag{19}$$

This function adopts the hyperbolic sinusoidal constitutive model commonly used for aluminum alloys[22]:

$$\dot{\varepsilon} = A[\sinh(\alpha\sigma^*)]^n \exp(\frac{-Q}{RT}) \tag{20}$$

Where Q is the strain activation energy, and T is the deformation temperature same as θ in Eq. (19).

The ideal elastic–plastic model is used for the liquid phase element. The elastic modulus is set the same as that of the solid phase. The yield stress σ_{yield} is minimized.

$$\Delta\bar{\varepsilon}_{\text{in}}^{t+\Delta t} = \begin{cases} 0 & \bar{\sigma}^{*t+\Delta t} \le \sigma_{\text{yield}} \\ \left(\bar{\sigma}^{*t+\Delta t} - \sigma_{\text{yield}}\right)/3G & \bar{\sigma}^{*t+\Delta t} > \sigma_{\text{yield}} \end{cases} \tag{21}$$

Where $\bar{\sigma}^{*t+\Delta t}$ is an intermediate parameter constructed during the iterative process, with its specific iterative steps the same as in [7]. The two-phase region is directly divided into a solid phase and a liquid phase. The liquid phase has a small solid-phase fraction fs, and the solid phase has a large fs value. A critical value $f_{s,c}$ is set up so that $f_{\text{s}} < f_{\text{s,c}}$ means the liquid phase, and $f_{\text{s}} > f_{\text{s,c}}$ means the solid phase.

There is a continuous movement process of the punch to maintain the pressure in the solidification process. The punch displacement was solved by using an iterative method as follows. First, an initial value was assumed for the punch displacement, and the stress field was solved at the first time step. Then, the total reaction force at the interface between the punch and the casting part was calculated and compared with the punch pressure to obtain an iteration difference. Such iterations were performed at each time step until the iteration difference was less than a critical value.

2.3 Prediction model of thermal cracking

Because squeeze casting is a solidifying process under pressure, the RDG criterion containing the pressure term is suitable for predicting the thermal cracking tendency in the squeeze casting process. In application of the RDG criterion, the strain rate term can be directly evaluated from the FEM simulation result of the solidification process. However, the secondary dendrite spacing term exists in a mesoscopic scale and hence cannot be directly calculated from the macroscopic model. The mesh size of the FEM model is in millimeter, while the computational size of the dendrite growth is in micron. Therefore, the FDM refinement method is needed to complete the bridge from the macroscopic scale to the mesoscopic scale .

The difference scheme of two-dimensional unsteady heat conduction is shown in Eq. (23). The equivalent specific heat capacity of the latent heat of crystallization is calculated by using the equivalent specific heat method

as follows:

$$c'_p = c_p - H\frac{\partial f_s}{\partial T} = c_p + \frac{H}{T_L - T_S} \tag{22}$$

$$T^{n+1}_{(i,j)} = \frac{1}{M_1}(T^n_{(i-1,j)} + T^n_{(i+1,j)}) + \frac{1}{M_2}(T^n_{(i,j-1)} + T^n_{(i,j+1)}) + (1 - \frac{2}{M_1} - \frac{2}{M_2})T^n_{(i,j)} \tag{23}$$

Where $T^n_{(i,j)}$ is the temperature at moment n and node (i, j), and

$$M_1 = \frac{\Delta x^2}{a\Delta t} \qquad M_2 = \frac{\Delta y^2}{a\Delta t} \qquad a = \frac{\lambda}{\rho c_p} \tag{24}$$

The subcooling degree and the temperature gradient were obtained by data processing of the local refined temperature field.

2.3.1 Dendrite growth simulation

The equiaxed crystal model of the binary alloy [15] based on the phase field method was adopted. The subcooling degree obtained from local refinement of the FDM was substituted into the phase field model. The phase field evolution equation containing anisotropic characteristics is given by

$$\begin{aligned}\frac{\partial \phi}{\partial t} = \mu\Gamma\left[-\frac{\partial}{\partial x}\left(\sigma\sigma'\frac{\partial \phi}{\partial y}\right) + \frac{\partial}{\partial y}\left(\sigma\sigma'\frac{\partial \phi}{\partial x}\right) + \nabla\cdot\left(\sigma^2\nabla\phi\right) - \frac{\phi(1-\phi)(1-2\phi)}{\omega^2}\right] \\ + \mu(T_m - T + m_l C_l)\frac{\phi(1-\phi)}{\omega}\end{aligned} \tag{25}$$

Where ϕ is an order parameter, μ linear kinetic coefficient, Γ Gibbs–Thomson coefficient, T temperature, T_m equilibrium melting temperature of pure substance, ml liquidus slope in the equilibrium phase diagram, and Cl equilibrium concentration in liquid. The anisotropic function is given by

$$\sigma(\theta, \theta_0) = 1 + \delta\cos[4(\theta - \theta_0)] \qquad \theta = \tan^{-1}\left(\frac{\partial\phi/\partial y}{\partial\phi/\partial x}\right) \tag{26}$$

The concentration evolution equation is given by

$$\frac{\partial C}{\partial t} = \nabla\cdot D[\nabla C + \frac{(1-k)C}{1-\phi+k\phi}\nabla\phi] \tag{27}$$

$$D = D_s + (D_l - D_s)\frac{1-\phi}{1-\phi+k\phi} \tag{28}$$

Where k is distribution coefficient, D_l diffusion rate of alloy elements in liquid, and D_s diffusion rate of alloy elements in solid.

The equation of the temperature field is given by

$$\frac{\partial T}{\partial t} = \alpha \cdot \nabla^2 T + \frac{L}{C_P}\frac{\partial \phi}{\partial t} \tag{29}$$

2.3.2 Thermal cracking criterion

The RDG criterion used in this paper treats the model of the thermal cracking process as interdendritic liquid metal feeding. If the feeding is incomplete during solidification, or if the interdendritic liquid metal pressure is less than the critical pressure, the cores of thermal cracking are formed. After the secondary dendrite spacing calculated by the phase field method and the strain rate calculated by the FEM solidification are input into the RDG criterion, the thermal cracking tendency is judged by using the following equation:

$$HSC_{RDG} = \frac{180\mu\Delta T}{G^2\lambda_2}(|\dot{\varepsilon}|\beta A + (1+\beta)B\dot{\varepsilon}\Delta T) - P_m \tag{30}$$

Where P_m is static pressure, G temperature gradient, μ metal liquid viscosity, λ_2 secondary dendrite spacing, β shrinkage factor, and $\dot{\varepsilon}$ strain rate. Moreover, $\Delta T = T_{mf} - T_{end}$. In Eq. (30),

$$A = \frac{1}{\Delta T}\int_{T_{end}}^{T_{mf}} \frac{f_s^2 dT}{(1-f_s)^2} \tag{31}$$

$$B = \frac{1}{\Delta T}\int_{T_{end}}^{T_{mf}} \frac{f_s^2 F_s(T) dT}{(1-f_s)^3} \tag{32}$$

$$F_s(T) = \frac{1}{\Delta T}\int_{T_{end}}^{T} f_s dT \tag{33}$$

Where fs is solid phase fraction.

3. Simulation results and analysis

3.1 Three-dimensional modeling

This paper simulates a squeeze casting bracket as an example. The part is shown in Fig. 1(a). The casting system is shown in Fig. 1(b). The casting material is ADC12 aluminum alloy. The metal mold material is H13 steel. Table 1 shows the thermal properties of ADC12. Table 2 shows the production process parameters.

.

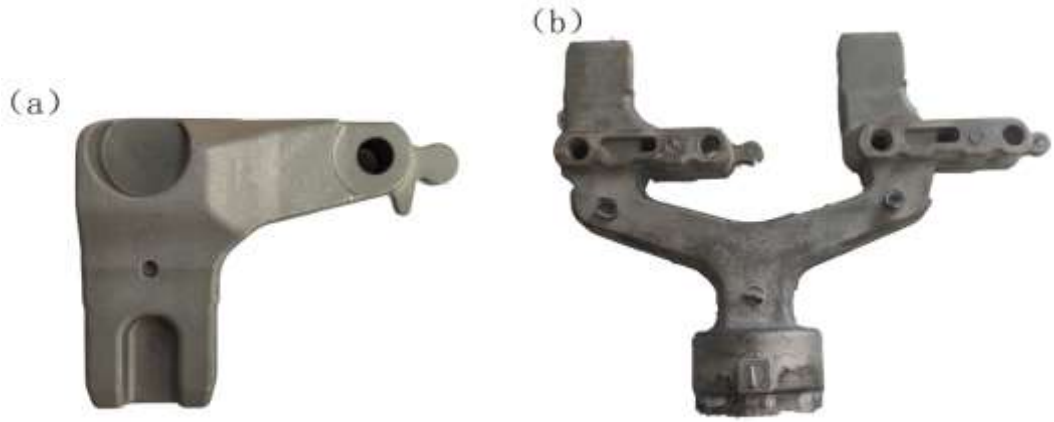

Fig.1. Bracket and its casting system

(a) Automobile bracket drawing

(b) Casting system drawing

Table 1 Properties of ADC12 aluminum alloy used in simulation

Parameter	Thermal conductivity [W/(m·K)]	Specific heat capacity [J/(kg·K)]	Density (kg/m3)	Solidus temperature (°C)	Liquidus temperature (°C)	Latent heat (J/kg)	Poisson's ratio
Value	96.0-96.2	963	2.64-2.67	525.8	607.5	389000	0.33

Table 2 Production process parameters

Parameter	Punch pressure (bar)	Punch velocity (m/s)	Pouring temperature (°C)	Punch temperature (°C)	Mold temperature (°C)	Holding time (s)
Value	130	0.23	670	200	200	15

3.2 Filling simulation results

The filling process simulated by using the SPH method is compared with the filling process simulated by the Procast method, as shown in Fig. 2. The Procast simulation is shown on the left, and the SPH simulation is shown on the right. The metal liquid was placed in an external die chamber in advance as shown in Fig. 2(a), and the metal liquid moved upward under the push of the punch. As shown in Fig. 2(b), the metal liquid accelerated from the large cross section to the small cross section, and the flow was split and moved to the both sides of the mold after the flow hit the wall. As shown in Fig. 2(c), the two flows on the both sides moved up along the wall until they reached the left and right sides of the wall. As shown in Fig. 2(d), the flows entered the both sides of the bracket. Due to different velocity directions on the both sides, filling occurred sequentially at the both sides. As shown in Figs. 2(e) and 2(f), the metal liquid surface first contacted the top wall and then fell down to fill the mold. Fig. 2(g) shows the status of completed filling.

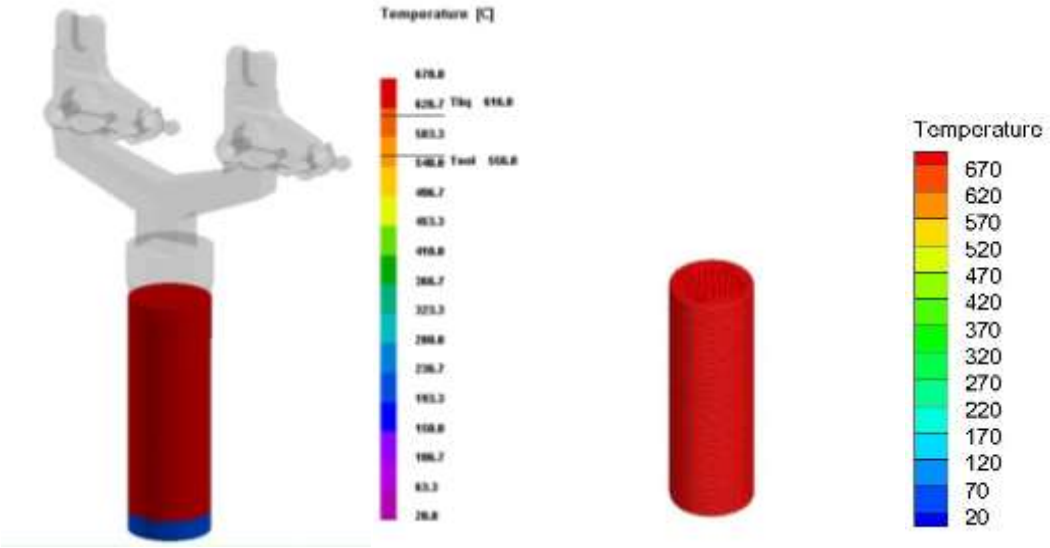
Temperature [C]
Temperature
670
620
570
520
470
420
370
320
270
220
170
120
70
20

(a) t=0 s

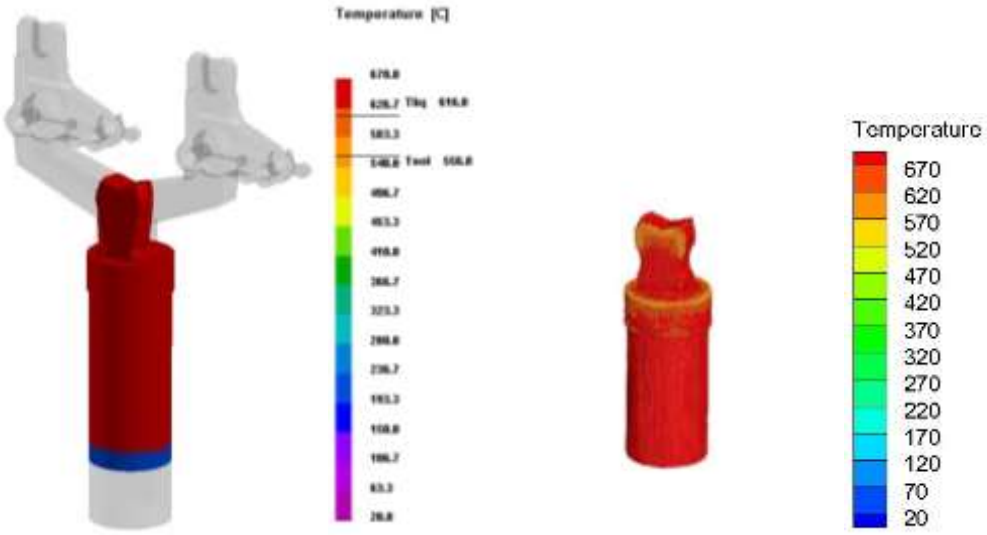
Temperature [C]
Temperature
670
620
570
520
470
420
370
320
270
220
170
120
70
20

(b) t=0.39 s

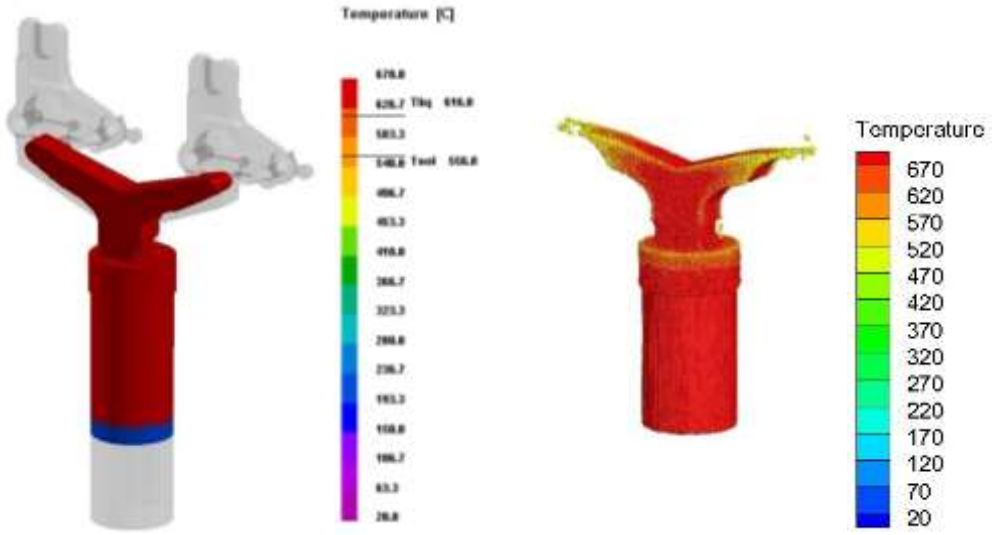

(c) t=0.47 s

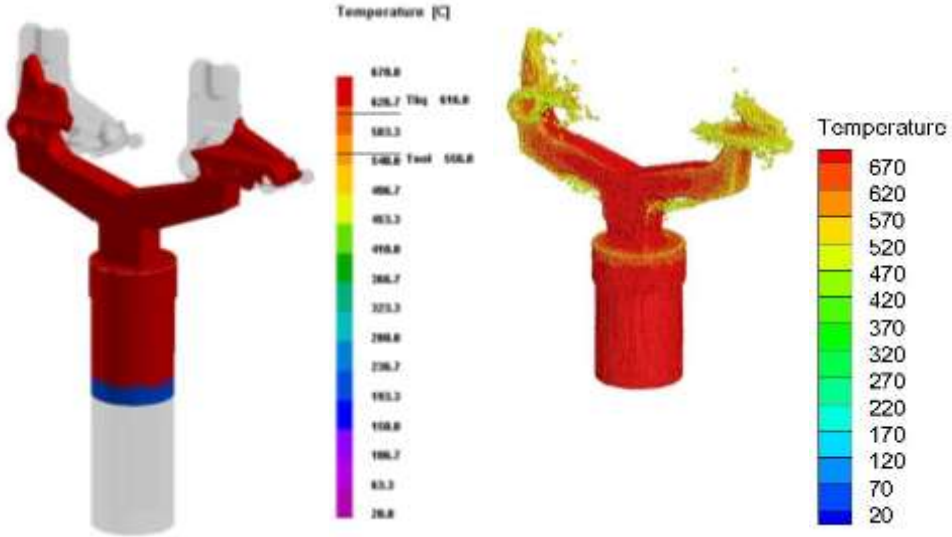

(d) t=0.59 s

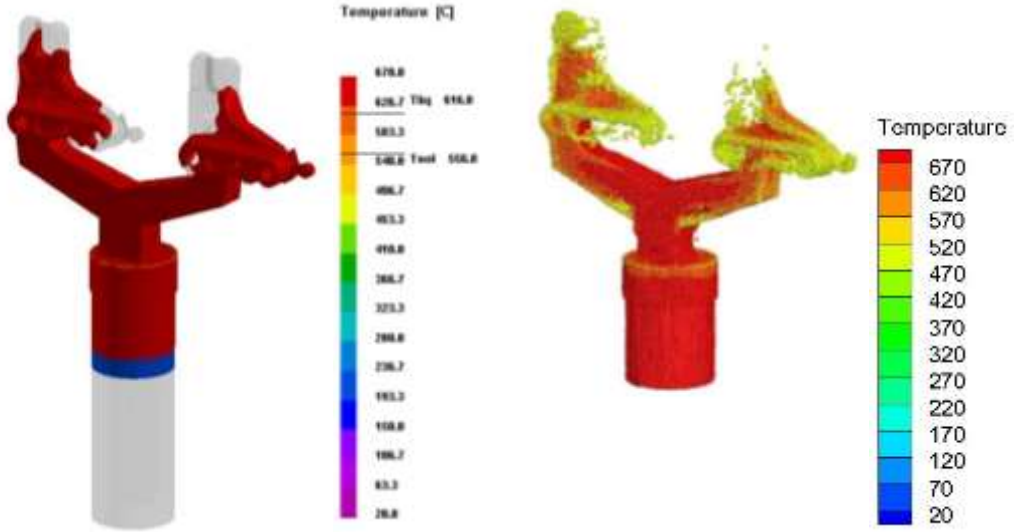

(e) t=0.67 s

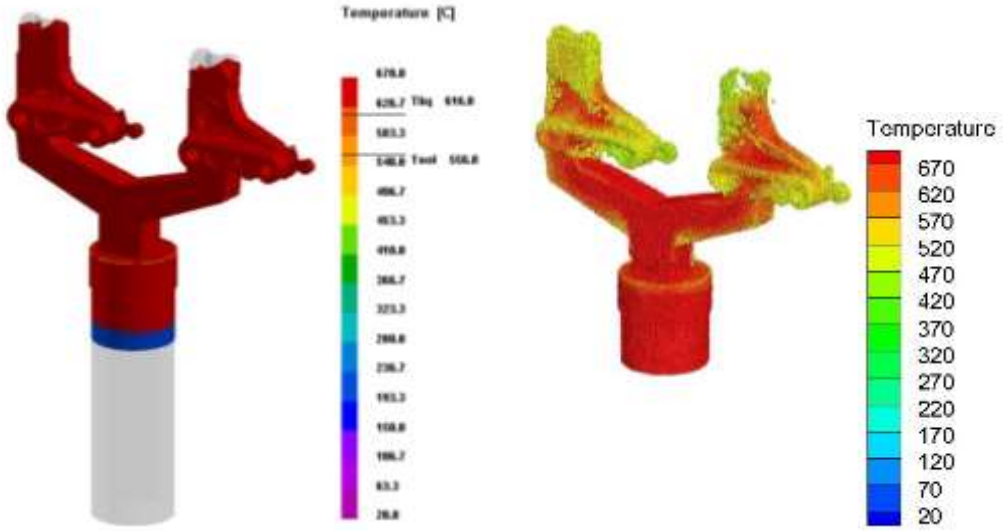

(f) t=0.78 s

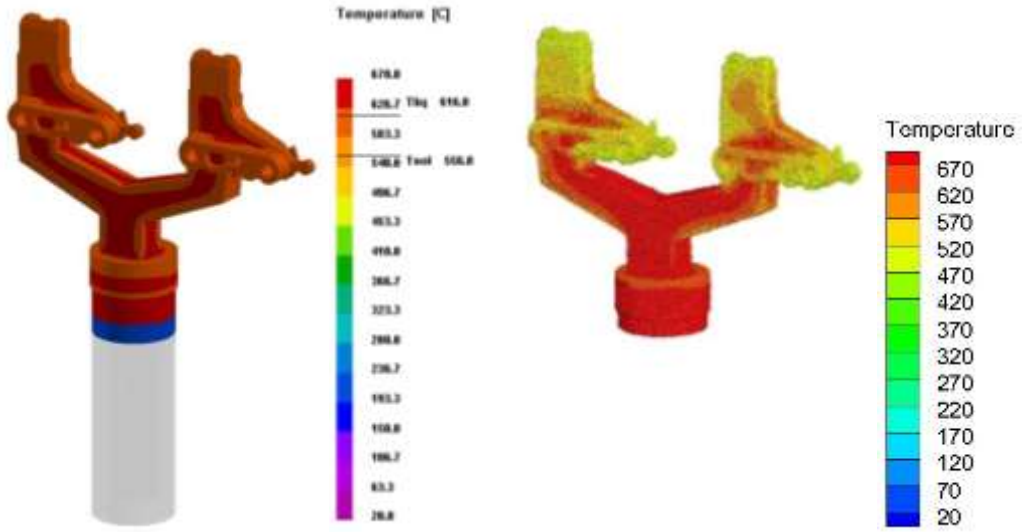

(g) t=0.94 s

Fig.2. Filling process simulation

As shown in Fig. 2(b), both the Procast and SPH results show a necking phenomenon, which was caused by the acceleration of the metal fluid under the impact of the squeeze action from the large cross section to the small cross section. Detailed velocity analysis is given later in Fig. 3. As shown in Fig. 2(c), the Procast and SPH results began to differ from that moment. The SPH particles impacted the wall under the action of the punch. The velocity in the z-axis direction was changed to the velocity in the x-axis direction. Liquid splash appeared at the most upfront end of the liquid surface. The temperature of the splashed particles decreased rapidly after they contacted the wall. In contrast, the Procast result does not show these phenomena. The reason for the difference is that the FEM cannot simulate liquid splash without adding node-separation coupling[23]. In comparison, the SPH method shows an advantage of simulating the squeeze casting and filling process. As shown in Fig. 2(f), the filling sequences in the Procast result and the SPH result are similar, but the SPH result better illustrates the details of liquid splash when the liquid's front segment contacted the mold wall. Fig. 2(g) shows the completion of the filling process. The temperature fields in the SPH result and the Procast result are very similar, validating the satisfactory accuracy of the SPH simulation of the temperature field for the filling process of squeeze casting.

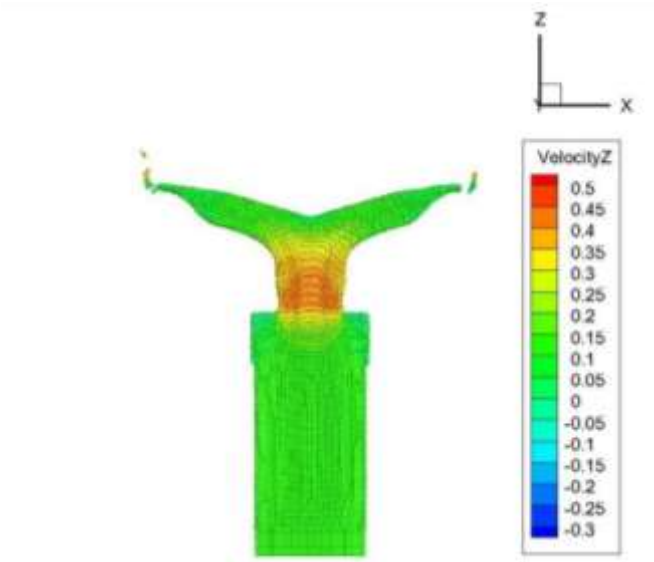

Fig.3. Cross section diagram of the axial velocity in the SPH result at 0.47 s

Fig. 3 shows the cross section diagram of the axial velocity distribution in the SPH result at 0.47 s. The particles at the edge accumulated before entering the small cross section from the large cross section. The central particles began to accelerate before entering the small cross section and reached the maximum velocity in the middle of the small cross section, and then slowed down rapidly. The particles continued to decelerate after leaving the small cross section till impacting the wall.

3.3 Prediction results of thermal cracking

The temperature field at the end of filling calculated by the SPH method was imported into the FEM program for solidification process simulation. The temperature field at the initial moment of the FEM simulation is shown in Fig. 4. The temperature of the flow passage was greater than that of the bracket. The part with the lower temperature of the flow passage is at the right-angle edge, and the shunt part had high temperatures due to continuous filling of the high-temperature metal liquid. The temperature in the bracket near the flow passage was higher, and the temperature far away from the flow passage was lower.

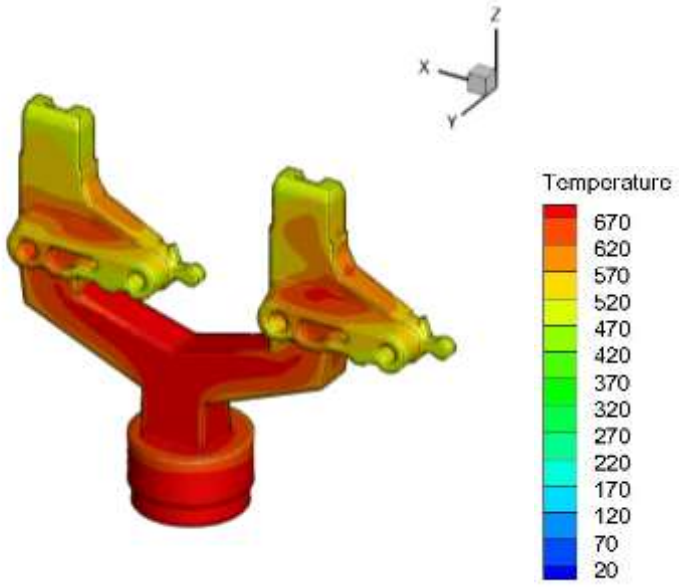

Fig.4. Temperature field at the initial moment of the FEM simulation

The uniform two-dimensional meshing technology was adopted without reducing simulation accuracy. To intuitively illustrate the thermal cracking tendency, the cross section with the largest strain rate difference between the maximum value and the minimum value was selected, as shown in Fig. 5. Certain points were selected from this cross section for subsequent FDM local refinement, dendrite growth simulation, and thermal cracking defect prediction.

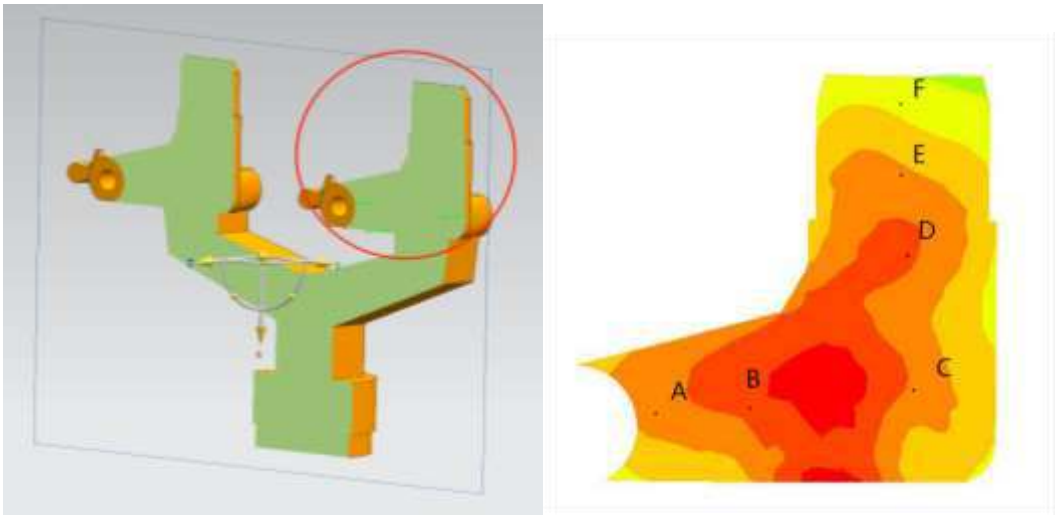

Fig.5. Vertical cross section along the y axis and points selection

The strain rate term in the RDG criterion was obtained from the FEM simulation result of the solidification process. The strain rate distribution in the cross section is shown in Fig. 6. Points C and D are located on the thin wall of the cross section, resulting in higher strain rates. However, points A and D had lower strain rates due to their later filling sequences and resulted positions on the thick wall. The secondary dendrite spacing term in the RDG criterion of thermal cracking needs to be simulated by using the phase field method. The refinement results were input into the phase field model to conduct simulation on dendrite growth. The parameters of the phase field model are shown in Table 3.

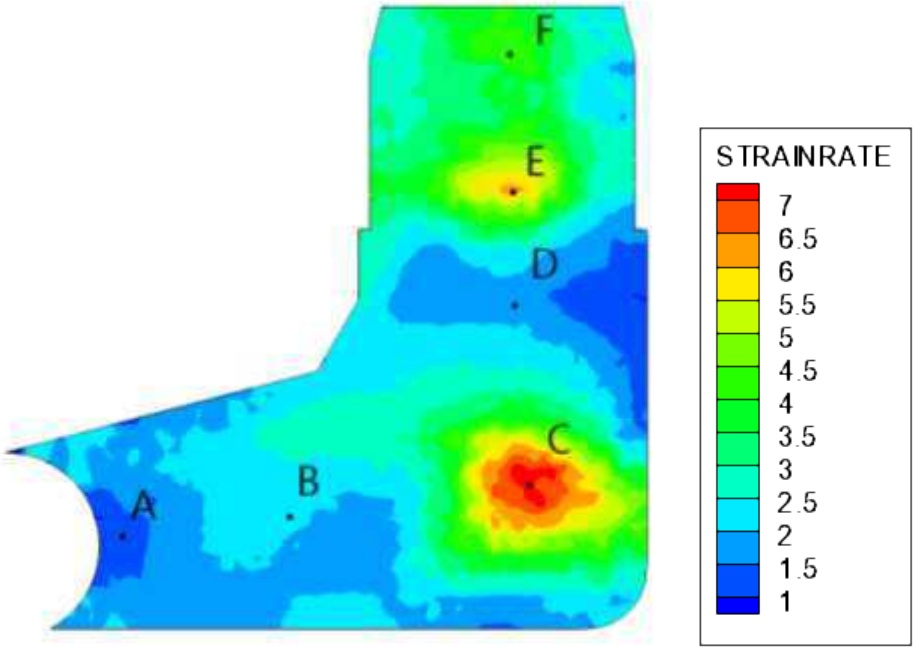

Fig.6. Strain rate field in the cross section at 10 s

Table 3 Parameters in the phase field model

Parameter	Value
Liquidus slope ml (K/W·t, pct)	–6.58
Diffusivity of alloy elements in liquid Dl (m2/s)	3×10–9
Diffusivity of alloy elements in solid Dl (m2/s)	1×10–12
Melting temperature of pure aluminum (°C)	660
Melting temperature of pure silicon (°C)	1410

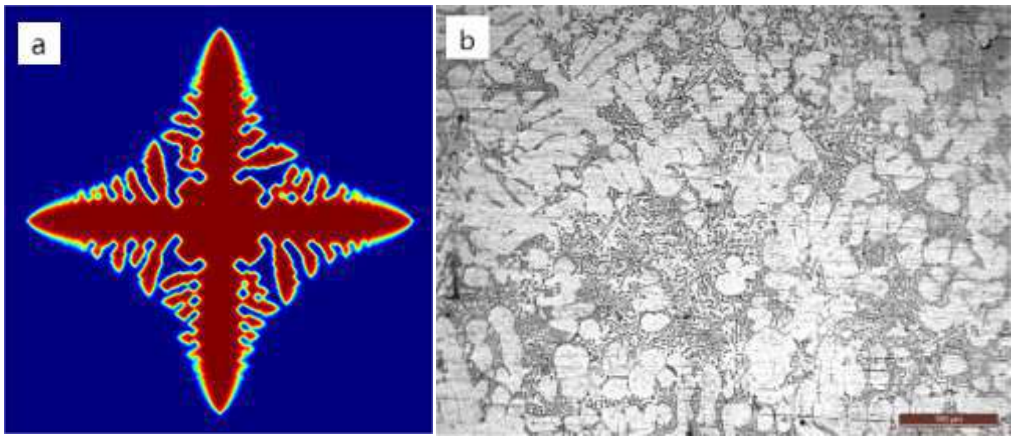

Fig.7. Comparison between simulation result of dendritic growth at point C and Microstructure at point C.

(a)Simulation result of dendritic growth at point C

(b) Microstructure at point C

The dendrite growth conditions were simulated successively at the selected points. The simulated secondary dendrite spacing data were imported into the RDG criterion to predict thermal cracking. Since point C had the highest strain rate in the cross section, it is selected for detailed interpretation here. Fig. 7(a) shows the simulation result of dendritic growth at point C. Fig. 7(b) shows the microstructure picture of point C under a holding pressure of 130 bar. The microstructure was composed of α-Al cells and (α+β) eutectic particles. The actual secondary dendrite spacing in Fig. 7(b) is 17.8 μm based on measurement. The simulation result after measurement in Fig. 7(a) is very similar to the experimental result.

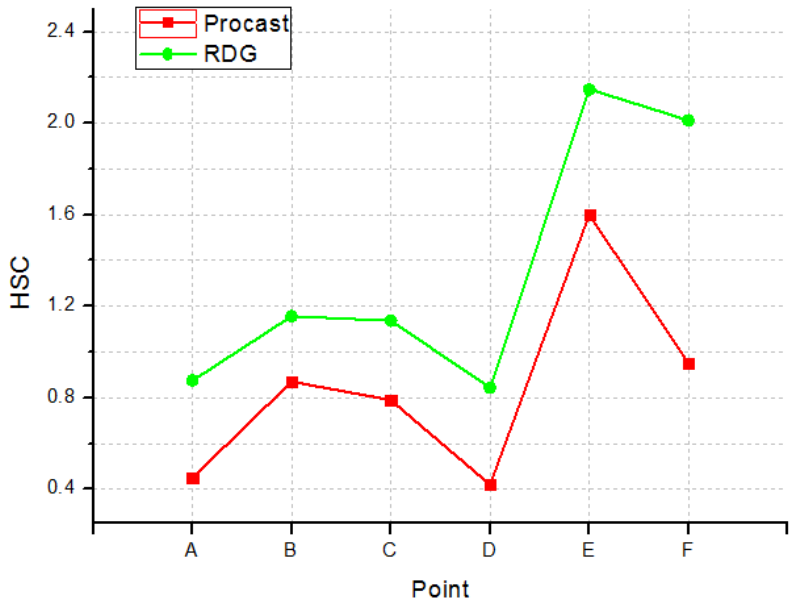

Fig.8. Comparison of thermal cracking tendency prediction between the RDG criterion and Procast

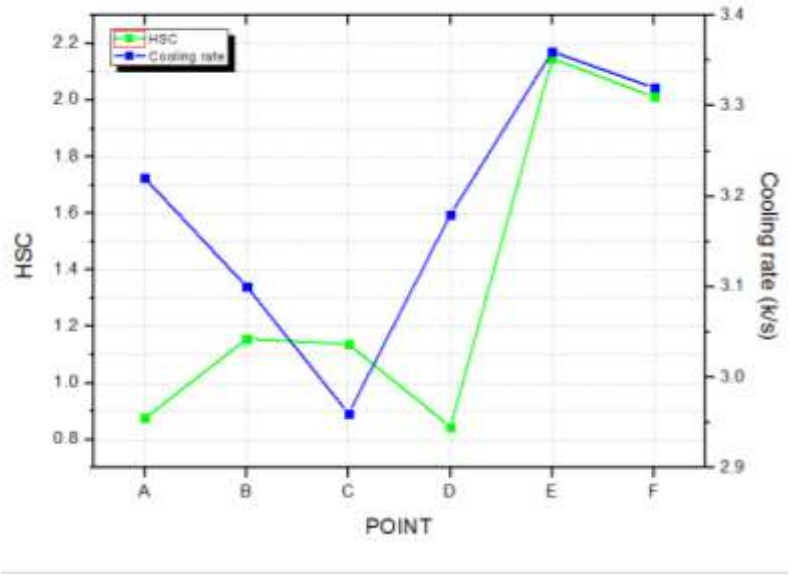

Fig.9. Comparison between thermal cracking tendency prediction based on the RDG criterion and cooling rate

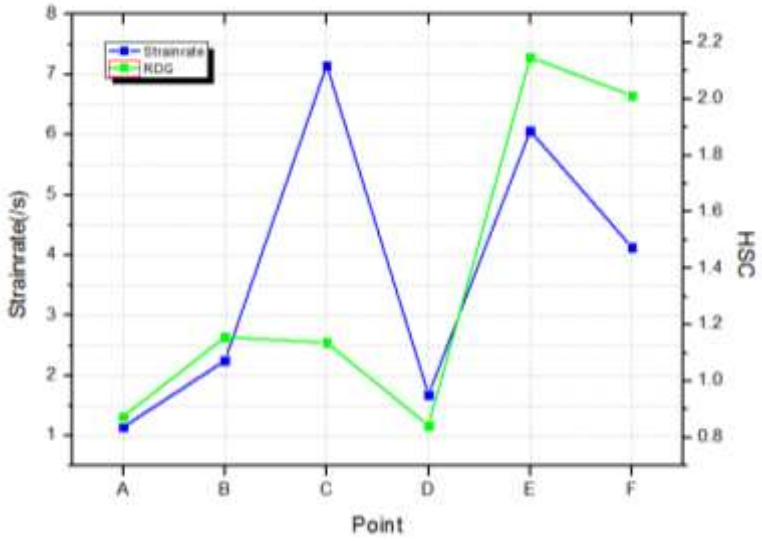

Fig.10. Comparison between thermal cracking tendency prediction based on the RDG criterion and strain rate

Fig. 8 shows the comparison of thermal cracking tendency prediction between the RDG criterion and Procast. The lowest and highest positions of thermal cracking tendency appeared at points D and E, respectively. The thermal cracking prediction results of the multi-scale multi-mathematical-model approach developed in this paper and the Procast method are similar in the overall trend, validating the satisfactory accuracy of the proposed approach in thermal cracking prediction of the squeeze casting process. However, the HSC value of the thermal cracking tendency calculated based on the RDG criterion is greater due to the static pressure in this paper. Fig. 9 shows the comparison between the thermal cracking tendency prediction based on the RDG criterion and the cooling rate. Fig.

9 shows that points B and C near the center of the bracket had lower cooling rates, while points A, E, and F near the edge of the bracket had higher cooling rates. When the metal liquid was closer to the low temperature wall, the cooling rate became higher. Fig. 10 shows the comparison between the thermal cracking tendency prediction based on the RDG criterion and the strain rate. Overall, the thermal cracking tendency increased when the strain rate increased. However, point C had the highest strain rate of 7.15/s, but its thermal cracking tendency was not high, being only 1.13729. This was because point C was close to the casting system and the dendrite gap was well complemented so that its cooling rate was as low as 2.96 K/s, as shown in Fig. 9. As a result, the influence of the high strain rate was offset. Similarly, point A had the lowest strain rate but a higher cooling rate. The effect of the low strain rate was offset by the high cooling rate, so that the thermal cracking tendency of point A was 0.875009, slightly greater than that of point D.

4. Conclusions

(1)The SPH method is advantageous in tracking the free surface and the moving interface and hence can be used to simulate the filling process of squeeze casting . Then, the simulation results at the end of filling were input into the FEM program as the initial condition to simulate the solidification process. The FEM program used the thermoelasto–viscoplastic constitutive model to fully simulate the three-phase deformation behavior of the squeeze casting process and the mechanical behavior. Because the RDG criterion contains the pressure term, it fits well the pressurized solidification process of squeeze casting and hence can be used to accurately predict the thermal cracking tendency of squeeze casting parts. The phase field method was used to conduct mesoscale simulations to obtain the secondary dendrite spacing term, which was then input into the RDG criterion together with the strain rate term calculated by the FEM to predict thermal cracking. This proposed approach of combining the phase field method with the RDG criterion provides a new way of thermal cracking prediction.

(2)In the filling process simulation, the SPH method proposed in this paper can better predict the flow field, the filling sequence, and liquid splashing details compared to the Procast method. The FEM program uses the thermoelasto–viscoplastic constitutive model to calculate the three-phase mechanical behavior. The simulation results show that the thin wall has a higher strain rate and the thick wall and the wall with a later filling sequence have lower strain rates, conforming with production practice. The secondary dendrite spacing and the strain rate simulated by the phase field method were input into the RDG criterion to predict the thermal cracking of squeeze casting. The thermal cracking prediction results given by the multi-scale multi-mathematical-model approach and the Procast method were compared. These two methods produced basically consistent results, validating the accuracy of the proposed approach. The comparison between the thermal cracking prediction and the strain rate shows that the thermal cracking tendency increases with an increase in strain rate. However, the local point C had the highest strain rate of 7.15/s, but its thermal cracking tendency was only 1.13729 due to the fact that under the influence of a

low cooling rate of 2.96 K/s the effect of the high strain rate on the increase in the thermal cracking tendency was offset.

Statements and Declarations

Funding

This work has been supported by the National Natural Science Foundation of China (No.51874209) and the Science and Technology Major Project of Shanxi Province (No. 20191102007).

Competing Interests

The authors have no relevant financial or non-financial interests to disclose.

Author Contributions

All authors contributed to the study conception and design. Material preparation, data collection and analysis were performed by [Yan Liu], [Tao-tao Ge], [Pei-lin Luo] and [Ming-yu Zhang]. Article checking was performed by [Xiao-feng Niu] and [Wei Zhou]. The first draft of the manuscript was written by [Zhan Zhao] and all authors commented on previous versions of the manuscript. All authors read and approved the final manuscript.

References

[1] Cleary PW, Ha J, Prakash M, Nguyen T. (2006)3D SPH flow predictions and validation for high pressure die casting of automotive components. Applied Mathematical Modelling. 30:1406-27. https://doi.org/10.1016/j.apm.2006.03.012

[2] Cleary PW, Savage G, Ha J, Prakash M. (2014)Flow analysis and validation of numerical modelling for a thin walled high pressure die casting using SPH. Computational Particle Mechanics. 1:229-43. https://doi.org/10.1007/s40571-014-0025-4

[3] Chang QM, Chen CJ, Zhang SC, Schwam D, Wallace JF. (2010)Effects of process parameters on quality of squeeze casting A356 alloy. International Journal of Cast Metals Research. 23:30-6. https://doi.org/10.1179/174313309x449309

[4] Li J, Sun Y, Wang Y, Sun J. (2021)Optimization of squeeze casting process of gearbox cover based on FEM and Box-Behnken design. The International Journal of Advanced Manufacturing Technology. 1-10. https://doi.org/10.1007/s00170-021-08099-8

[5] Jonas J, Sellars C, Tegart WM. (1969)Strength and structure under hot-working conditions. Metallurgical

Reviews. 14:1-24. https://doi.org/10.1179/mtlr.1969.14.1.1

[6] Santhanam S. (2000)An elastic-viscoplastic constitutive model for the hot-forming of aluminum alloys. Journal of materials science. 35:3647-54. https://doi.org/10.1023/A:1004882001651

[7] Zhu W, Han ZQ, Liu BC. (2009)THERMOMECHANICAL MODELING OF SOLIDIFICATION PROCESS OF SQUEEZE CASTING II. Numerical Simulation and Experimental Validation. Acta Metallurgica Sinica. 45:363-8. https://doi.org/10.1016/S1003-6326(09)60084-4

[8] Hatami N, Babaei R, Dadashzadeh M, Davami P. (2008)Modeling of hot tearing formation during solidification. Journal of Materials Processing Technology. 205:506-13. https://doi.org/10.1016/j.jmatprotec.2007.11.260

[9] Clyne T, TW C. (1981)The influence of composition on solidification cracking susceptibility in binary alloy systems.

[10] Kou S. (2015)A criterion for cracking during solidification. Acta Materialia. 88:366-74. https://doi.org/10.1016/j.actamat.2015.01.034

[11] Rappaz M, Drezet JM, Gremaud M. (1999)A new hot-tearing criterion. Metallurgical and Materials Transactions A. 30:449-55. https://doi.org/10.1007/s11661-999-0334-z

[12] Kobayashi R. (1993)Modeling and numerical simulations of dendritic crystal growth. Physica D: Nonlinear Phenomena. 63:410-23. https://doi.org/10.1016/0167-2789(93)90120-P

[13] Warren JA, Boettinger WJ. (1995)Prediction of dendritic growth and microsegregation patterns in a binary alloy using the phase-field method. Acta Metallurgica et Materialia. 43:689-703. https://doi.org/10.1016/0956-7151(94)00285-P

[14] Battaglioli S, Robinson A, McFadden S. (2017)Axisymmetric front tracking model for the investigation of grain structure evolution during directional solidification. International Journal of Heat and Mass Transfer. 115:592-605. https://doi.org/10.1016/j.ijheatmasstransfer.2017.07.095

[15] Asle Zaeem M, Yin H, Felicelli SD. (2013)Modeling dendritic solidification of Al–3%Cu using cellular automaton and phase-field methods. Applied Mathematical Modelling. 37:3495-503. https://doi.org/10.1016/j.apm.2012.08.005

[16] Gingold RA, Monaghan JJ. (1977)Smoothed particle hydrodynamics: theory and application to non-spherical stars. Monthly notices of the royal astronomical society. 181:375-89. https://doi.org/10.1093/mnras/181.3.375

[17] Zhang C-b, Di D-n, Chen X-w, Wen K. (2020)Characteristics structure analysis on debris cloud in the hypervelocity impact of disk projectile on thin plate. Defence Technology. 16:299-307. https://doi.org/10.1016/j.dt.2019.09.011

[18] Lattanzio J, Monaghan J, Pongracic H, Schwarz M. (1986)Controlling penetration. SIAM Journal on Scientific and Statistical Computing. 7:591-8.

[19] Monaghan JJ. (2000)SPH without a tensile instability. Journal of computational physics. 159:290-311. https://doi.org/10.1006/jcph.2000.6439

[20] Hu L, Hong-Fu Q, Fu-Zhen C, Ya-Wei H, Shu-Jia F. (2015)A new boundary treatment method in smoothed particle hydrodynamics. ACTA PHYSICA SINICA. 64.

[21] J. M, Melenk, and, I., Babuka. (1996)The partition of unity finite element method: Basic theory and applications. Computer Methods in Applied Mechanics and Engineering. 139:289-314. https://doi.org/10.1016/S0045-7825(96)01087-0

[22] Han ZQ, Zhu W, Liu BC. (2009)THERMOMECHANICAL MODELING OF SOLIDIFICATION PROCESS OF SQUEEZE CASTING I. Mathematic Model and Solution Methodology. Acta Metallurgica Sinica. 45:356-62. https://doi.org/10.1016/S1003-6326(09)60084-4

[23] Komori K. (2014)Simulation of stationary crack during blanking using node separation method. Procedia Engineering. 81:1102-7. https://doi.org/10.1016/j.proeng.2014.10.205